Tumor-Selective Gene Expression in a Hepatic Metastasis Model after Locoregional Delivery of a Replication-Competent Retrovirus Vector

Kei Hiraoka, Takahiro Kimura, Christopher R. Logg, and Noriyuki Kasahara

Abstract

Purpose: Replication-competent retrovirus (RCR) vectors have been shown to achieve highly efficient and tumor-restricted replicative spread and gene transfer *in vivo* after direct intratumoral injection in a variety of primary cancer models. In this setting, the intrinsic inability of retroviruses to infect postmitotic normal cells, combined with their unique ability to persist through stable integration, allow further transduction of ectopic tumor foci as the infected cancer cells migrate. However, i.v. delivery of RCR vectors has never been tested previously, particularly in an immuno-competent tumor model.

Experimental Design: We combined optical imaging, flow cytometry, and molecular analysis to monitor RCR vector spread after administration via locoregional infusion in a hepatic metastasis model of colorectal cancer.

Results: Robust RCR replication was first confirmed in both human WiDr and murine CT26 colorectal cancer cells *in vitro*, with transduction levels reaching >90% in <12 days after virus inoculation at multiplicities of infection of 0.01 to 0.1. *In vivo*, infusion of RCR supernatant into the portal circulation resulted in progressive and significant transduction of multifocal intrahepatic CT26 tumors in syngeneic mice, averaging about 30% but with up to 60% transduction in some tumors within 4 weeks. However, immunohistochemistry and quantitative PCR analysis showed no evidence of RCR spread to adjacent normal liver or to any other normal tissues.

Conclusions: Our results thus show that locoregional infusion of RCR vectors can be used to deliver therapeutic genes selectively to tumor cells in the liver while sparing normal hepatocytes and without dissemination to extrahepatic normal tissues.

Colorectal cancer is still one of the leading causes of cancer-related death (1). The liver is the most common site of distant metastasis due to the direct flow of blood from the intestinal tract to the liver via the portal system, and liver metastases will develop in 60% of patients with colorectal cancer. Of these, surgical resection may result in long-term survival or cure in 30% who present without metastasis to extrahepatic sites. However, the 5-year survival rate after surgical resection remains only about 30% due to the high frequency of recurrence after hepatic resection (2–4).

In clinical trials of gene therapy for cancer, among the most commonly used gene delivery vehicles have been replication-defective retroviral vectors; however, transduction efficiencies have been insufficient for clinical use due to the inability of replication-defective viral vectors to diffuse throughout the entire tumor mass (5, 6). Current strategies to improve tumor transduction efficiency include the use of replication-competent instead of replication-defective viral vectors. Theoretically, the use of replicating viruses would be more efficient, as each transduced tumor cell will itself become a producer cell, generating more viral progeny, thereby amplifying the effect of the initial inoculum. A variety of tumors selectively replicating oncolytic viruses are being developed for oncolytic virotherapy of various solid cancers. However, although clinical trials have shown some efficacy and safety (7–12), the possibility of premature clearance by immune responses (13, 14) or nonspecific replication in normal cells (15–17) still needs to be more thoroughly evaluated.

Replication-competent retrovirus (RCR) vectors of the type used in the present study have been developed based on murine leukemia virus (MLV) as a novel vehicle for cancer gene therapy (18–20). These vectors have been found to be highly stable, capable of replicating without observable deletions through multiple serial infection cycles in culture (20) and can achieve highly efficient gene delivery to solid tumors *in vivo* (18). We have shown previously that, whereas transduction efficiency of replication-defective wild-type MLV vector was only 1.2%, RCR vector could achieve >90% transduction of s.c. injected glioma with almost same titer of virus (21). Compared with other replicating virus systems, RCR vectors exhibit unique

characteristics, including intrinsic selectivity for actively dividing cells and noncytolytic replication leading to stable integration in the target cell. These properties contribute to selective and persistent replication in tumors, and we and others have shown previously that RCR vectors could achieve efficient and tumor-restricted gene transfer and propagation, resulting in significant therapeutic benefit after direct intratumoral injection (21–24).

Whereas direct intratumoral injections could be used clinically for gene delivery to a few localized tumor foci, for example by ultrasound-guided percutaneous injection in the context of metastatic spread of colorectal cancer to the liver, a more practical solution for multifocal metastatic disease might be locoregional infusion of virus vectors via portal vein or hepatic artery. In previous studies, although significant therapeutic efficacy has been reported after locoregional infusion of retrovirus producer cells for immunocytokine gene transfer (25), the actual transduction efficiency with replication-defective retrovirus vector supernatant (4×10^5 to 5×10^5 total colony-forming units) has been reported to be <5% in 0% to 2% of metastatic tumors, and even with infusion of virus producer cells, the median transduction efficiency was reported to be on the order of 5% to 10% of tumor cells within a given lesion (25). Therefore, in the present study, we tested the replication kinetics, transduction efficiency, and tumor-selectivity of RCR vectors by locoregional administration via the portal system in a syngeneic mouse model of intrahepatic multifocal colorectal cancer metastasis. This represents the first study to examine locoregional delivery of RCR vectors, as well as the use of this vector system in an orthotopic model of gastrointestinal cancer, and the first use of optical imaging to monitor the spread of RCR vector spread *in situ*.

Materials and Methods

Cell lines and RCR vector plasmid. Transformed human embryonic kidney cell line 293T, human colon adenocarcinoma cell line WiDr, and BALB/c-derived murine colon adenocarcinoma cell line CT26 were obtained from American Type Culture Collection (Manassas, VA) and maintained in a humidified atmosphere with 5% CO2 in DMEM, MEM, and RPMI 1640, respectively, each supplemented with 10% fetal bovine serum and 1% penicillin-streptomycin.

The plasmid pACE-GFP has been described previously (21) and is a modification of RCR vector plasmid pAZE-GFP, which contains a full-length replication-competent amphotropic MLV provirus with an IRES-GFP cassette inserted between the *env* gene and 3′-untranslated region (20). In pACE-GFP, the U3 region of the 5′ long terminal repeat was replaced by the cytomegalovirus promoter to increase the initial level of viral mRNA transcription and RCR vector production on transient transfection of the plasmid. To develop pACE-CD, the IRES-GFP cassette of pACE-GFP was replaced with an IRES-CD cassette, which was amplified by PCR from the plasmid pCR-Blunt-CD, kindly provided by Dr. P. Roy-Burman (Department of Pathology, University of Southern California, Los Angeles, CA).

Virus production, titer determination, and analysis of replication kinetics in vitro. For production of the ACE-GFP virus, 293T cells were transiently transfected with plasmid pACE-GFP using LipofectAMINE 2000 (Invitrogen Life Technologies, Carlsbad, CA) and replenished with serum-free medium 8 hours after transfection. After incubation for an additional 48 hours, the supernatant medium was harvested, filtered through a 0.45-μm syringe filter, and stored frozen at −80°C. Polybrene (4 μg/mL; Sigma, St. Louis, MO) was added for all infections in culture. To determine viral titers, a precounted number of cells were infected

with serial dilutions of viral supernatant, incubated for 24 hours, after which 50 μmol/L 3′-azido-3′-deoxythymidine (Sigma) was added to prevent virus spread. After an additional 24 hours, the cells were trypsinized and analyzed for green fluorescent protein (GFP) expression on a Coulter EPICS flow cytometer (Beckman Coulter, Fullerton, CA). The viral titer was calculated as described previously (21) and represented as transducing units (TU) per milliliter.

For analysis of replication kinetics in colorectal cancer cells *in vitro*, virus vector stock at multiplicity of infection (MOI) of 0.01 or 0.1 was used to infect WiDr or CT26 cells at 20% confluency. At serial time points after virus infection, the cells were trypsinized, one fourth was replated, and the remainder was analyzed for GFP expression by flow cytometry. When the CT26 cells had reached ~100% transduction with ACE-GFP, this stably transduced cell population (CT26.GFP) was maintained for further experiments.

In vitro *cytotoxicity assay.* Cell viability was determined using a tetrazolium dye conversion [3-(4-5-dimethylthiazol-2-yl)-5-(3-carboxymethoxyphenyl)-2-(4-sulfophenyl)-2H-tetrazolium salt (MTS)] assay (Promega, Madison, WI). To assess drug cytotoxicity, triplicate wells containing CT26 or WiDr cells (2×10^3 per well) were cultured in 96-well plates with 1 mmol/L 5-fluorocytosine (5FC). On day 5, dye conversion was read using an ELISA plate reader at 490 nm following the 2 hours of reaction at 37°C. Cytotoxicity was determined by calculation of the absorbance of viable cells as measured against wells containing no 5FC. Drug cytotoxicity experiments were confirmed on each transduced cell line in at least three independent experiments.

Subcutaneous tumor and orthotopic liver metastasis models. Six-to eight-week-old female nude mice (Charles River Laboratories, Inc., Wilmington, MA) and female BALB/c mice [University of California at Los Angeles (UCLA) Division of Experimental Radiation Oncology animal facility] were bred and maintained in accordance with institutional guidelines under specific pathogen-free conditions, and all studies were conducted under protocols approved by the UCLA Animal Research Committee.

For s.c. tumor models, cell suspensions of WiDr (1×10^6/100 μL) or CT26 (5×10^4/100 μL) in HBSS were injected into the right dorsal flanks of nude mice or BALB/c mice, respectively. One week later, ACE-GFP (1×10^4 TU/100 μL) was given by direct intratumoral injection, and the tumors were dissected at different time points for analysis.

To establish a standard curve for fluorescence imaging of s.c. tumors, uninfected parental CT26 cells were mixed with CT26.GFP cells at various ratios (0-100%), and these CT26 cell mixtures (5×10^4 cells) in 100 μL HBSS were s.c. injected into each mouse. Two weeks later, the s.c. tumors were excised and analyzed by fluorescence imaging and flow cytometry as described below.

A syngeneic mouse model of colorectal cancer metastasis to the liver was also established as described previously (26), with minor modifications, by infusion of tumor cells into the portal system via intrasplenic injection. Briefly, after making a left subcostal incision under isoflurane anesthesia, CT26 tumor cells (5×10^4) in 200 μL HBSS were inoculated by intrasplenic injection through a 30-gauge needle followed by hemostasis for 5 minutes and wound closure. Three days after tumor cell inoculation, following anesthesia and a second laparotomy, ACE-GFP vector (2×10^4 TU/200 μL) was also given via intrasplenic injection, after which splenectomy was done.

Optical imaging and flow cytometric analyses of tumor transduction in vivo. GFP fluorescence in s.c. and liver tumors dissected at different time points, as well as other extratumoral normal tissues, was examined by optical imaging using a Xenogen-IVIS cooled CCD optical system (Xenogen IVIS, Alameda, CA). Gray-scale background photographic images of the tissues were overlaid with color images of emitted fluorescent light using Living Image software (Xenogen) and IGOR-PRO Image analysis software (Wave Metrics, Lake Oswego, OR).

Following optical imaging, tumors were minced and extraneous tissue was removed under sterile conditions. Samples were digested with collagenase/dispase (1 mg/mL; Roche Diagnostics, Mannheim, Germany) by incubation for 2 hours at 37°C, and the dissociated cells

were passed through a 100-μm cell strainer, pelleted by low speed centrifugation, and resuspended in PBS. Half of the cells were analyzed by flow cytometry to further quantitate GFP expression, and the remainder was placed in explant culture.

Immunohistochemical analysis. Livers frozen in ornithine carbamyl transferase (Sakura Tek, Torrance, CA) were cryosectioned (10 μm) at four different levels and fixed with 4% paraformaldehyde for 10 minutes. All incubations were done at room temperature. After endogenous peroxidase activity was blocked with 3% hydrogen peroxide for 10 minutes, the slides were washed, and nonspecific binding was blocked with 10% normal goat serum for 30 minutes. Tissue sections were then incubated with rabbit anti-GFP polyclonal antibody (Abcam, Inc., Cambridge, MA) diluted 1:200 with 1% bovine serum albumin for 90 minutes, washed in PBS followed by biotinylated secondary antibody, avidin-biotin horseradish peroxidase complex, and diaminobenzidine substrate according to the manufacturer's specifications (Vectastain avidin-biotin complex method Elite kit, Vector Laboratories, Burlingame, CA), counterstained with Hematoxylin QS (Vector Laboratories), and mounted.

Quantitative real-time PCR analysis of vector biodistribution. Genomic DNA was isolated from excised tissues (liver tumor, lung, small intestine, colon, kidney, and bone marrow) of transduced and untransduced animals using the DNeasy Tissue kit (Qiagen, Inc., Valencia, CA). To detect integrated RCR sequences, quantitative real-time PCR was done in a 25 μL reaction mixture containing genomic DNA from liver tumor or tissues of ACE-GFP-infected mice, 12.5 μL of 2× Taqman Universal PCR Master Mix (PE Applied Biosystems, Foster City, CA), 300 nmol/L each primer, and 100 nmol/L fluorogenic probe. Amplifications were carried out in duplicate using the ABI Prism 7700 sequence detector (PE Applied Biosystems); after initial denaturation (10 minutes at 95°C), amplification was done with 40 cycles of 15 seconds at 95°C and 60 seconds at 60°C. To calculate retrovirus copy number in the samples, a reference curve was prepared by amplifying serial dilutions of pACE-GFP plasmid in a background of genomic DNA from untransduced normal bone marrow cells and by plotting C_t values against the input plasmid. The threshold for vector detection was determined by a control sample with no plasmid. The primers and probe for analysis of vector copy number were designed to target the 4070A amphotropic envelope gene [4070A, 5'-GCGGACCCG-GACTTTTGA-3'(forward), 5'-ACCCCGACTTTACGGTATGC-3' (reverse), and FAM-CAGGGCACACGTAAAA-NFQ (probe)]. Mouse β-actin was also quantified as an internal control gene in each reaction [β-actin, 5'-GGTCGTACCACAGGCATTGT-3' (forward), 5'-CTCGTAGATGGGCA-CAGTGT-3' (reverse), and FAM-CCCGTCTCCGGAGTCC-NFQ (probe)].

Statistical analysis. Statistical analyses were done with Student's *t* test to determine significance. Coefficient of determination (r^2) values >0.9 were defined as a strong correlation. *P* values <0.05 were considered statistically significant in all analyses, which were done with Prism 4 statistical software (GraphPad Software, San Diego, CA).

Results

RCR vector replication and transgene transmission in human and murine colorectal cancer cell lines. The MLV-based RCR vector ACE-GFP (21) contains an encephalomyocarditis IRES-GFP cassette inserted precisely at the *env* stop codon, 3'-untranslated region boundary (Fig. 1A). Compared with previously described replication-competent MLV vectors containing transgene inserts in the U3 region of the 3' long terminal repeat (27–29), this configuration greatly improves genomic stability over multiple replication cycles (19, 20). Virus stocks were prepared by transient transfection of 293T cells with pACE-GFP plasmid, and the titer of initial vector stocks as determined by flow cytometric analysis for GFP

expression, after infection of human (WiDr) and murine (CT26) colorectal cancer cell lines in the presence of 3'-azido-3'-deoxythymidine to inhibit virus replication, ranged between 2×10^5 and 1×10^6 TU/mL.

Replication kinetics and transgene transmission efficiency at low MOI were then examined by flow cytometric monitoring of GFP expression at serial time points after infection with ACE-GFP in the absence of 3'-azido-3'-deoxythymidine. In WiDr human colorectal cancer cells, the initial percentage of GFP-positive cells was already ∼25% by day 3 after infection at a MOI of 0.1 and increased rapidly to reach 97% by day 9. After infection of WiDr cells at a MOI of 0.01, a lag phase of about 3 days was followed by logarithmic increase in GFP expression, which reached >90% by day 12 (Fig. 1B, *left*). Subsequently, GFP expression in the fully transduced WiDr cell populations remained stable for at least several months. WiDr cells were also infected with another MLV-based RCR vector, ACE-CD, expressing the yeast *cytosine deaminase* (*CD*) suicide gene, at a MOI of 0.1 in parallel with ACE-GFP produced under identical conditions. After an 18-day culture period, >95% transduction by ACE-GFP was confirmed in the parallel control cells by flow cytometry. As the CD enzyme converts the nontoxic prodrug 5FC into the chemotoxin 5-fluorouracil directly inside infected tumor cells, *in vitro* cytotoxicity was then examined by MTS assay after exposure of transduced cells to the 5FC prodrug (Fig. 1B, *right*). Whereas ACE-GFP-transduced cells showed no growth inhibition after 5FC treatment, the cell viability of ACE-CD-transduced cells was reduced by >80% after 5 days of exposure to the prodrug. Similar results were obtained after ACE-GFP transduction of the CT26 murine colorectal cancer cell line, although the increase in the percentage of GFP-positive cells was somewhat slower, taking 12 days to reach 92% at a MOI of 0.1 and showing a lag phase of a little under 6 days followed by logarithmic increase to >90% by day 15 at a MOI of 0.01 (Fig. 1C, *left*). As with WiDr cells, the fully transduced CT26 cell populations showed stable GFP expression for at least several months. To confirm further RCR production from this stably transduced cell population (CT26.GFP), fresh CT26 cultures were infected with conditioned cell culture supernatant from the CT26.GFP cells. Subsequently, the percentage of GFP-positive cells increased and reached >95% in a same kinetics with that in the initial experiment (data not shown). Also as above, >85% reduction in cell viability was observed on exposure to 5FC after CT26 cells were fully transduced with ACE-CD, whereas CT26 cells transduced with ACE-GFP in parallel maintained >90% viability after 5FC treatment (Fig. 1C, *right*). Thus, the RCR vector could achieve robust, dose-dependent spread, associated with efficient and stable transmission of transgenes, in both human and murine colorectal cancer cell lines, as confirmed by GFP transmission and suicide gene activity.

RCR vector mediates intratumoral spread of GFP in s.c. colorectal cancer models. We first evaluated the *in vivo* transduction efficiency and replicative spread of the ACE-GFP vector in s.c. tumor models established by inoculation of 1×10^6 WiDr human colorectal cancer cells in nude mice and 5×10^4 CT26 murine colorectal cancer cells in syngeneic BALB/c mice, respectively; the more aggressive growth rate of the CT26 tumors necessitates a smaller initial inoculum. One week after establishment, each tumor was injected with 1×10^4 TU total dose of the ACE-GFP vector. At weekly intervals, cohorts of

tumors were excised and disaggregated into single-cell suspensions by collagenase treatment and immediately analyzed by flow cytometry to evaluate the percentage of GFP-positive cells within each tumor. In s.c. WiDr tumors, the percentage of GFP-positive cells averaged 16% at 1 week and reached >50% by 2 weeks after virus injection. In s.c. CT26 tumors, the percentage of GFP-positive cells increased >7-fold between weeks 2 and 3 after virus injection, from <3% to ~20% of the entire tumor mass (Fig. 2). These results are consistent with the previous results of *in vitro* RCR replication kinetics in each cell line, with more rapid transmission of the GFP transgene observed in the human colorectal cancer cell line. Although even higher levels of tumor transduction could presumably be achieved starting from the same initial RCR dose if virus spread was allowed to continue, further monitoring was not possible, as both WiDr and CT26 tumors had grown to the size limit of 2,500 mm³ as defined by institutional guidelines by 2 to 3 weeks after virus injection.

Comparison of optical imaging and flow cytometry in CT26 s.c. tumor model. We also used a CCD optical imaging system to examine the GFP signal from RCR-transduced CT26 tumors. First, to determine the sensitivity, specificity, and linearity of

GFP fluorescence signals detected by CCD optical imaging, s.c. tumors consisting of uninfected parental CT26 cells mixed with ACE-GFP-transduced CT26 cells (CT26.GFP) in various ratios (0-100%) were established in BALB/c mice and then excised and analyzed by optical imaging 2 weeks later. All of the GFP fluorescence images were taken under the same conditions 2 weeks after tumor establishment. After imaging analysis, each tumor was digested and analyzed by flow cytometry to compare the percentage of GFP-positive cells with the imaging results. The GFP fluorescence signal intensity and the percentage of GFP-positive cells in each tumor were shown in Fig. 3. The comparative results show the strong correlation between the signal intensities and the percentage of GFP-expressing cells in the tumors ($r^2 = 0.91$; $P < 0.0001$).

Locoregional infusion of ACE-GFP vector supernatant results in widespread and progressive transduction of multifocal CT26 liver metastases. We then tested the ability of the RCR vector to transduce hepatic mestastases *in vivo* after direct locoregional infusion of virus supernatant in syngeneic BALB/c mice. This results in the rapid development of multifocal tumors in the liver that generally prove fatal about 4 weeks later. Three days after tumor establishment by portal infusion, a total dose of

Fig 1. *A*, design of RCR vectors. This vector contains a full-length replication-competent amphotropic MLV proviral sequence, in which an IRES-GFP or IRES-CD (*CD* suicide gene) cassette has been inserted between the *env* gene and 3′-untranslated region, and the U3 region of the 5′ long terminal repeat has been replaced by the cytomegalovirus (*CMV*) promoter. *B* and *C, in vitro* replication kinetics and suicide gene activity in human colorectal cancer cell line WiDr (*B*) or murine colorectal cancer cell line CT26 (*C*). To examine replication kinetics, both cell lines were infected with ACE-GFP at a MOI of 0.01 or 0.1 and analyzed for GFP expression by flow cytometry every 3rd day after virus infection for a period of 21 days (*B* and *C, left*). To examine suicide gene activity, 18 days after infection with ACE-CD, or ACE-GFP in parallel (MOI, 0.1), the viability of transduced cells with (+) or without (−) 5-day exposure to the prodrug 5FC was measured by MTS assay (*B* and *C, right*). IRES, internal ribosome entry site.
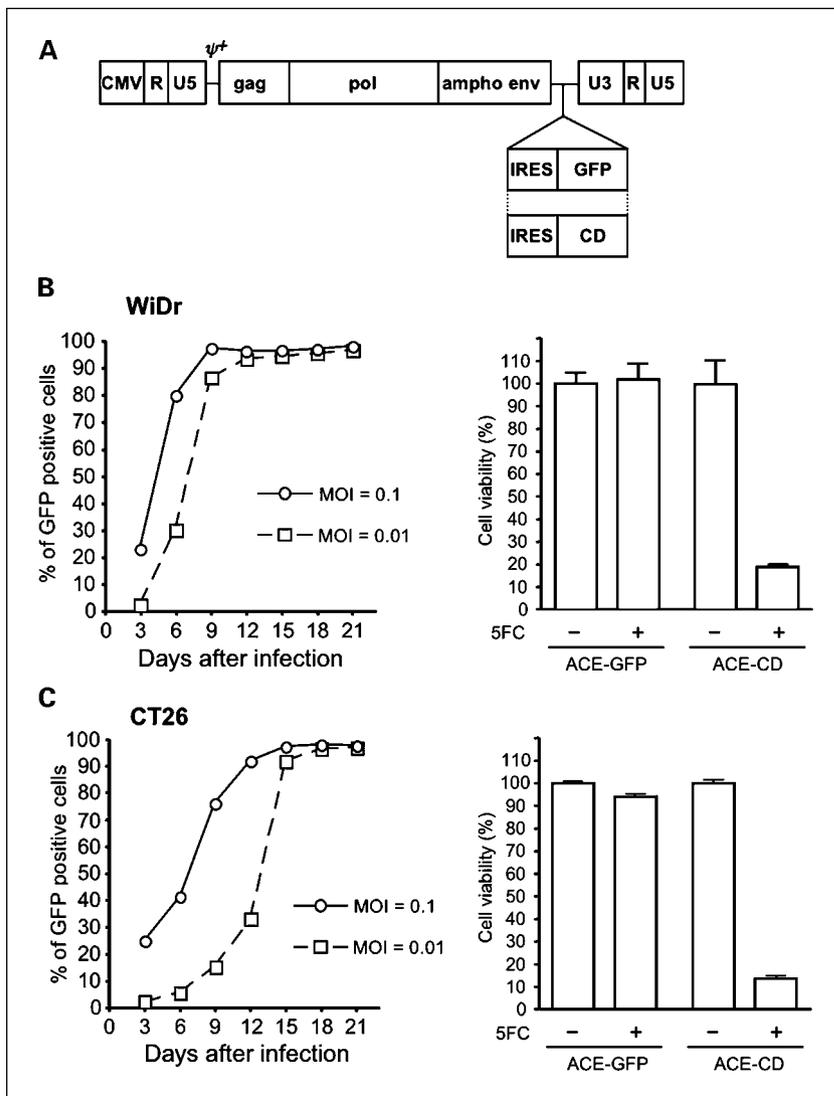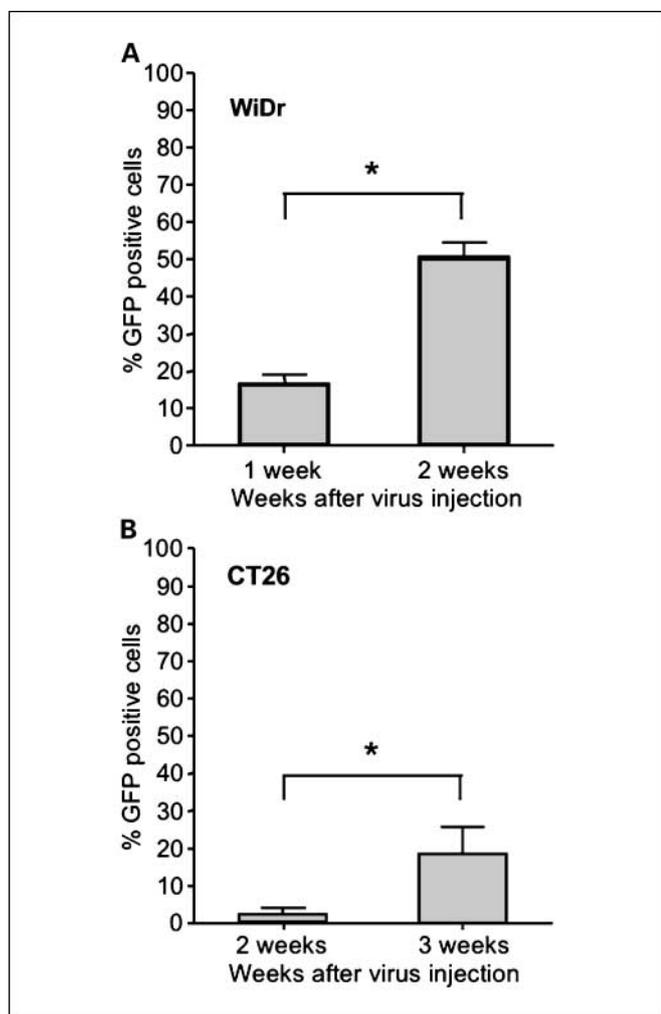
Fig. 2. Spread of ACE-GFP in s.c. tumor models of colorectal cancer. ACE-GFP (1×10^4 TU/100 μL) was injected into each tumor 1 week after tumor establishment. At weekly intervals after virus injection, individual tumors were dissected, enzymatically disaggregated, and immediately analyzed by flow cytometry for GFP expression. Columns, mean ($n = 4$ for each group at each time point); bars, SD. *, $P < 0.05$.

2×10^4 TU ACE-GFP virus supernatant in 200 μL total volume was infused by the same route, and 2 and 4 weeks later, the excised livers were analyzed by optical imaging. Two weeks after virus infusion, only very small areas of weak GFP expression could be observed in some tumors by fluorescence imaging. However, by 4 weeks after injection, there were significant increases in the intensity and area of GFP expression that could be observed in multiple tumor sites (Fig. 4A and B).

Tumors larger than 5 mm in diameter were randomly dissected from the liver tissue of mice, digested with collagenase, and immediately analyzed by flow cytometry to evaluate the percentage of ACE-GFP-transduced cells. Despite the development of multifocal liver tumors in this metastatic colon cancer model, the transduction efficiency of RCR-mediated GFP marker gene transfer averaged 2.9% (range, 0-11%) and 30% (2.8-60%) in liver tumors at 2 and 4 weeks after virus infusion, respectively (Fig. 4C). Thus, there was again a positive trend toward increasing transduction levels over time, although the CT26 hepatic metastases were lethal within 4 to 5 weeks and so later time points could not be examined.

Analysis of ACE-GFP biodistribution. To better visualize ACE-GFP distribution within the liver, tissue sections were examined by immunohistochemistry using an anti-GFP antibody. Consistent with the results from optical imaging and flow cytometry, tumor masses showing strong positive staining could be observed at 4 weeks after virus injection (Fig. 5). However, there was no staining for GFP in the normal liver parenchyma, suggesting that viral replication was well restricted to the rapidly dividing cells within the tumor foci. Similarly, no signals were detected in extratumoral normal tissues by fluorescence imaging or standard PCR methods (data not shown). For more rigorous detection of any possible RCR vector spread to normal organs, quantitative real-time PCR analysis of genomic DNA extracted from peritumoral normal liver tissue, bone marrow, lung, kidney, small intestine, and colon was done using primers and probe sequences specific for the 4070A amphotropic envelope (Table 1). This method was determined to be sensitive enough to detect 35 copies of the RCR provirus per 5×10^4 cellular genomes (0.07%). As expected, proviral RCR signals were strongly detected in genomic DNA from ACE-GFP-transduced tumor tissues. However, no detectable signals were observed in genomic DNA from uninvolved normal liver tissue or any other extratumoral normal tissues after ACE-GFP tumor transduction.

Discussion

In the present study, we used both optical imaging as well as flow cytometric analysis to examine GFP expression in multifocal tumors after locoregional delivery of a RCR vector in a syngeneic model of colorectal cancer metastasis to the liver. This vector was capable of efficient *in vitro* transduction in both human and murine colorectal cancer cell lines, reaching >90% transduction levels within <2 weeks in culture starting from
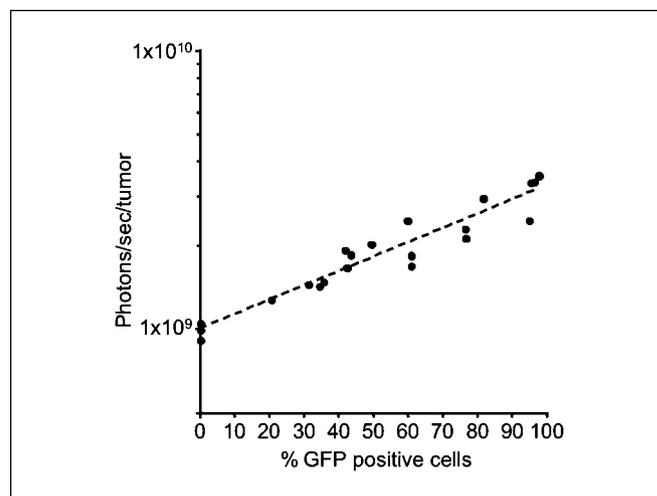

Fig. 3. Signal intensity of GFP fluorescence imaging and the percentage of GFP-expressing cells in ACE-GFP-transduced tumors. To analyze the correlation between the obtained GFP fluorescence signals and the actual percentage of GFP-expressing cells, the standard s.c. tumors for GFP fluorescence imaging were established. Parental CT26 cells were mixed with CT26.GFP cells transduced with ACE-GFP, in various ratios (0-100%), and then the mixture of CT26 cells were s.c. injected into mice. Two weeks later, the s.c. tumors were excised and analyzed for GFP fluorescence imaging and for GFP expression by flow cytometry. The signal intensities strongly correlated with the percentage of GFP-expressing cells in the tumors ($r^2 = 0.91$; $P < 0.0001$).

Fig. 4. Locoregional infusion model. *A,* 3 days after splenic injection of CT26 tumor cells, ACE-GFP vector was injected by the same route. Two and 4 weeks after virus injection, the livers were excised for fluorescence imaging for GFP expression in the liver tumors. No virus vector was injected into the control mice (*No vector*). *B,* fluorescence signal per liver tumor of the liver surface was quantified at each time point. *C,* transduction of metastatic liver tumors with ACE-GFP vector. The dissected tumors were dissociated and analyzed by flow cytometry for GFP expression at each time point. ACE-GFP vector was injected into spleen 3 days after tumor cell inoculation. The intensity of GFP signal and the percentage of GFP-expressing cells significantly increased in liver tumor model. Points, mean of four mice. *, $P < 0.05$.
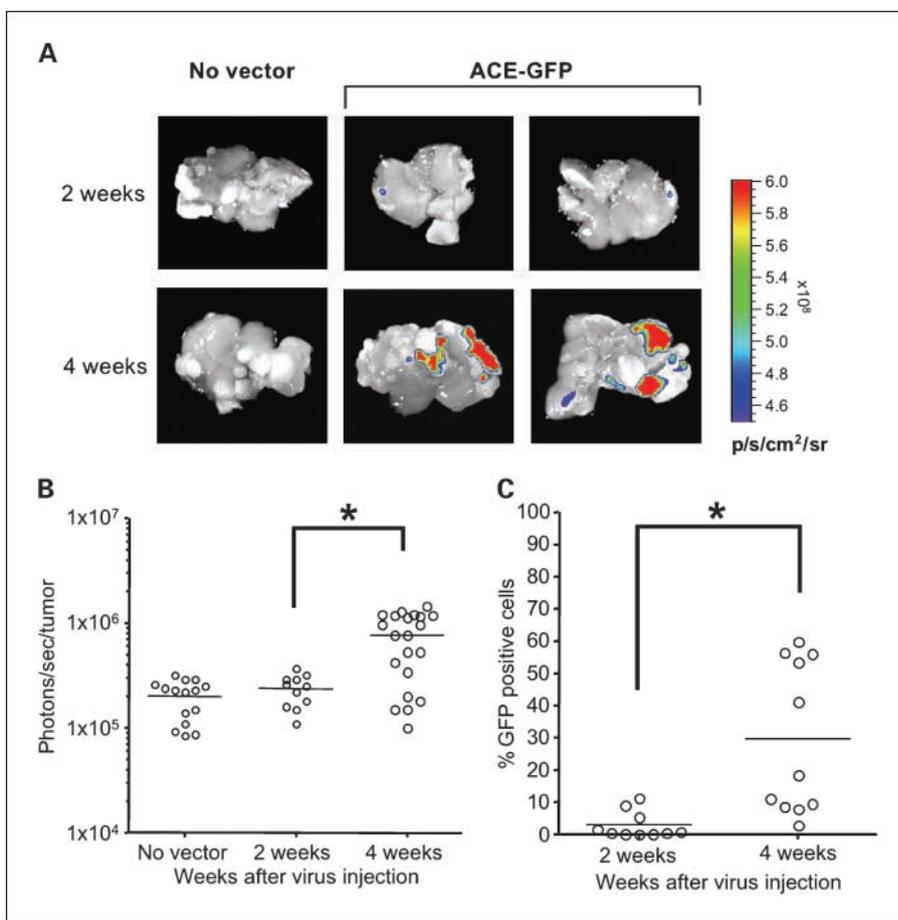
MOIs of 0.1 to 0.01. *In vivo*, comparative analysis showed that optical imaging allowed rapid and convenient examination of overall GFP expression and distribution, and the results obtained with this modality were generally highly well correlated and quite consistent with the more precise quantitation afforded by flow cytometry.

These experiments also showed that locoregional infusion of RCR vector supernatant via the portal system can mediate specific and significant transduction of multiple metastasized liver tumors, even in immunocompetent hosts. The average transduction efficiency of randomly harvested liver tumors >5 mm in size was about 30%, with transgene expression in some tumors reaching up to 60% by 4 weeks after injection of 2×10^4 total RCR vector supernatant. In contrast, in prior studies using 20-fold higher levels of replication-defective retrovirus vector supernatant delivered via the same route, transduction could be detected in only 2% or less of all metastatic intrahepatic tumors and did not account for >5% of the tumor cells in any positive tumor (25).

One of the main limitations of this model was the restricted observation period due to the highly aggressive nature of CT26 tumor growth; multifocal tumor growth in the liver resulted in lethality within 4 to 5 weeks after tumor cell inoculation. However, in clinical situations, generally, tumor growth in many human malignancies can be slower than that of experimental tumors originating from cancer cell lines, and this is predicted to affect the replication kinetics of RCR spread within the tumor mass. Allowing a longer period for intra-

tumoral spread after initial viral injection, or administering higher dose of virus to achieve a higher level of initial transduction and shorten the lag phase, could enable transduction of larger numbers of cancer cells. However, it should also be noted that the retrovirus has the capability to permanently integrate into the genome of the host tumor cell and will continue to produce progeny virus transcribed from the integrated copy whether the infected tumor cell is itself dividing or not. Thus, once any tumor cells have been infected, these will serve as a stable source for continued virus production so that the virus will still be available when adjacent uninfected tumor cells eventually divide even if this occurs slowly.

There was also a considerable heterogeneity of the level of transduction among multiple liver tumors; this is also consistent with previous experiments using intrasplenic infusion for retroviral vector supernatant and producer cell delivery in similar hepatic metastasis models (25), which represents one of the few studies to rigorously examine the transduction levels achieved in multifocal tumor lesions via this mode of delivery. In this previous report, even when 1×10^6 retroviral producer cells were introduced via intrasplenic infusion, the majority of metastatic tumor foci showed a median level of transduction within any given tumor of only 5% to 10%, with about 90% of transduced tumors showing transduction levels of <30% (25). With RCR vector infusion, we observed a bimodal distribution of intratumoral transduction efficiency, with almost half of the tumors showing transduction levels of 30% or more but half of
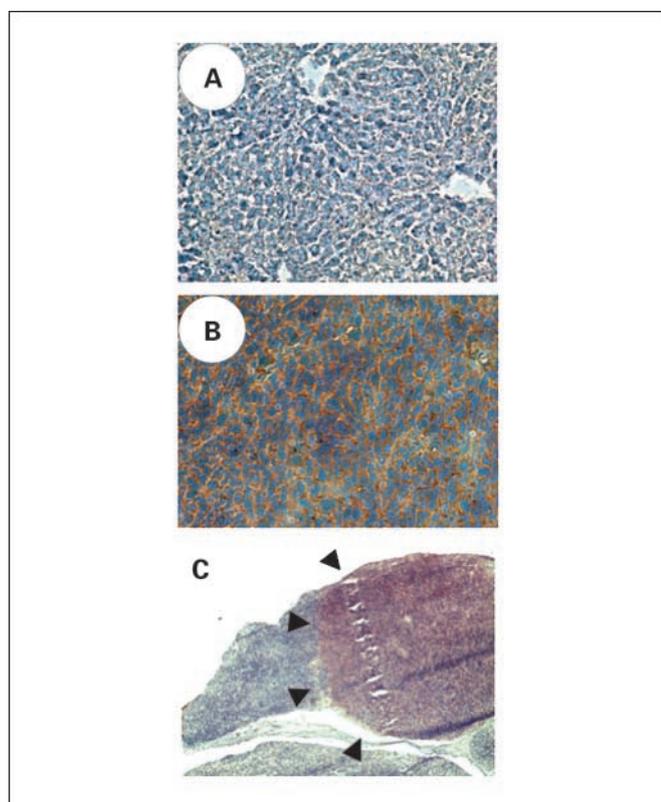
Fig. 5. Immunohistochemical analysis of GFP expression on sections of liver tumors from ACE-GFP-injected mice. Four weeks after virus injection, frozen liver sections were stained with GFP-specific antibodies. Brown, positive staining. Normal part of the liver (original magnification, ×400; *A*) or positive stained tumor [original magnifications, ×400 (*B*) and ×10 (*C*)]. Arrows, positive stained tumor nodule.

the tumors showing transduction levels of 10% or less. This suggests that tumor establishment in this model is so aggressive that some of the multifocal tumors that formed had very few ACE-GFP-transduced cells to begin with and showed the usefulness of optical imaging to understand the topological distribution of vector spread compared with overall average transduction levels determined from flow cytometry. This high level of heterogeneity in the transduction level among different tumors also suggests that the RCR vector itself is incapable of spreading through normal liver parenchyma from tumor to tumor.

One possible reason of this heterogeneity is that, despite a more even distribution of the initial virus inoculum, due to the aggressive nature of this model, secondary tumors might have formed from the initial tumor nodules, some of them at very early time points after RCR vector injection, before significant virus spread had occurred. Because a small difference of the level of initial transduction in each tumor would result in a large difference during the logarithmic replication phase, it would take longer time to achieve higher level of transduction of tumors with low levels of initial transduction, such as secondary tumor. Another possibility, which can occur commonly in human disease, is the formation of tumor thrombi (i.e., clumps or small nodules of cancer cells in the lumen of the portal vein that might obstruct the transfer of injected retrovirus to tumor foci distal to the obstruction). To increase the amount of virus particles transferred to the targeted tumor sites, transcatheter hepatic arterial infusion of therapeutic virus by a vascular interventional radiology procedure might enable us to avoid loss of virus activity by leading the tip of the catheter selectively into the section of intrahepatic artery supplying the tumor vasculature. In addition, to improve the transduction efficiency of replication-defective MLV vectors in liver tumors, instead of using a single dose of virus-containing supernatant, injection of conventional retroviral vector producer cells has been reported to achieve major improvements in transduction efficiency (25, 30, 31), and a similar approach could be used with RCR vector producer cells.

For the clinical use of replication-deficient retrovirus vectors, the possible production of RCR has been a major concern because of the risk of pathogenic insertion of virus genome into host genomic DNA. Theoretically, most normal cells could not be infected with RCR because of the intrinsic selectivity of MLV solely for actively dividing cells. However, the possibility still remains that some normal dividing cells infected with RCR vector might increase the risk of insertional mutagenesis. Certainly, the RCR vector described in this study also has the potential to transduce actively dividing normal cells, such as endothelial cells, fibroblasts, lymphocytes, and hepatocytes. However, despite the use of an untargeted RCR vector in this study, we could not detect the transgene sequence by PCR analysis in any normal tissues, including lung, liver, small intestine, colon, kidney, and bone marrow. Consistent with this result, it has been reported previously that after i.v. injection of wild-type MLV, although low levels of transduction were detected in bone marrow and spleen in nude mice by

Table 1. Biodistribution of RCR vector 4 weeks after locoregional virus infusion in immunocompetent hepatic metastasis model

		Copy number of RCR vector/5×10^4 cells					
Mouse	**Tumor**	**Bone marrow**	**Liver**	**Lung**	**Kidney**	**Small intestine**	**Colon**
ACE-GFP-1	2960	—*	—	—	—	—	—
ACE-GFP-2	2995	—	—	—	—	—	—
ACE-GFP-3	7890	—	—	—	—	—	—

NOTE: Genomic DNA, extracted from liver tumor, bone marrow, normal liver, lung, kidney, small bowel, and colon tissue of ACE-GFP-infected mice, was analyzed by quantitative real-time PCR as described in Materials and Methods. As an internal control, each sample was also amplified with mouse β-actin-specific primers.
*Not detectable (detection limit was 35 copies/5×10^4 cells).

real-time PCR, there was no transduction observed in any tissue after injection into immunocompetent mice (24). This is consistent with the classic reports of MLV-induced leukemogenesis, which occurs after virus inoculation in immunologically immature newborn mice but not in fully immunocompetent adult mice (32), and studies conducted before the initiation of the first gene therapy trials in humans showing that wild-type amphotropic MLV is nonpathogenic in normal immunocompetent primates after i.v. injection (33), bone marrow transplantation (34), or even producer fibroblast implantation with immunosuppression (33). Furthermore, administration of anti-retroviral drugs, such as 3′-azido-3′-deoxythymidine, could effectively eliminate viral contamination of bone marrow and spleen in nude mice (24). Additionally, with suicide gene therapy using RCR vectors, prodrug administration would not only kill infected cancer cells but also unintentionally transduced noncancerous cells.

Additional mechanisms to enhance tumor selectivity could be added by making alterations to the virus construct. To improve the selectivity of retroviral vector targeting, major advances have been made in the modification of retroviral envelope (35, 36) or replacement of the transcriptional control elements within the U3 region of the long terminal repeat with tissue-specific promoters (37–39). Envelope modifications that allowed specific adhesion of conventional replication-defective retroviruses to exposed collagen in tumor neovasculature were reported to improve therapeutic efficacy in liver metastasis models (40–44). We have shown previously high specificity and effective replication of RCR vector transcriptionally targeted to the prostate epithelium by replacement of the U3 region with sequences from the probasin promoter (18). For colon cancer, the carcinoembryonic antigen promoter (40–44) might be a suitable candidate for transcriptional targeting.

Our results thus show that RCR vectors can efficiently replicate and achieve significant levels of tumor transduction even in immunocompetent hosts, and locoregional infusion of RCR vectors via the splenic vein can mediate highly efficient transduction of multifocal liver tumors without detectable spread to normal tissues. Therefore, RCR vectors may represent a highly suitable vehicle for delivering therapeutic genes selectively to metastatic tumor cells in the liver while sparing normal hepatocytes. Furthermore, stable integration of RCR vectors in the host cell genome may allow greater persistence of therapeutic gene expression compared with many other replicating oncolytic viruses, which often rapidly kill the host cell during infection but achieve only transient tumor suppression. We are now further evaluating the therapeutic efficacy of RCR vector-mediated suicide gene and immunocytokine gene transfer for treatment of colorectal cancer metastasis.

Acknowledgments

References

1. Jemal A, Murray T, Ward E, et al. Cancer statistics, 2005. CA Cancer J Clin 2005;55:10–30.
2. Bentrem D, DeMatteo R, Blumgart L. Surgical therapy for metastatic disease to the liver. Annu Rev Med 2004;56:139–56.
3. Mayer-Kuckuk P, Banerjee D, Kemeny N, Fong Y, Bertino J. Molecular therapies for colorectal cancer metastatic to the liver. Mol Ther 2002;5:492–500.
4. Wagner JS, Adson MA, Van Heerden JA, Adson MH, Ilstrup DM. The natural history of hepatic metastases from colorectal cancer. A comparison with resective treatment. Ann Surg 1984;199:502–8.
5. Rainov NG. A phase III clinical evaluation of herpes simplex virus type 1 thymidine kinase and ganciclovir gene therapy as an adjuvant to surgical resection and radiation in adults with previously untreated glioblastoma multiforme. Hum Gene Ther 2000;11:2389–401.
6. Ram Z, Culver KW, Oshiro EM, et al. Therapy of malignant brain tumors by intratumoral implantation of retroviral vector-producing cells. Nat Med 1997;3:1354–61.
7. Nemunaitis J, Ganly I, Khuri F, et al. Selective replication and oncolysis in p53 mutant tumors with ONYX-015, an E1-55kD gene-deleted adenovirus, in patients with advanced head and neck cancer: a phase II trial. Cancer Res 2000;60:6359–66.
8. Reid T, Galanis E, Abbruzzese J, et al. Hepatic arterial infusion of a replication-selective oncolytic adenovirus (dl1520): phase II viral, immunologic, and clinical endpoints. Cancer Res 2002;62:6070–9.
9. Reid T, Galanis E, Abbruzzese J, et al. Intra-arterial administration of a replication-selective adenovirus (dl1520) in patients with colorectal carcinoma metastatic to the liver: a phase I trial. Gene Ther 2001;8:1618–26.
10. Nemunaitis J, Khuri F, Ganly I, et al. Phase II trial of intratumoral administration of ONYX-015, a replication-selective adenovirus, in patients with refractory head and neck cancer. J Clin Oncol 2001;19:289–98.
11. Khuri F, Nemunaitis J, Ganly I, et al. a controlled trial of intratumoral ONYX-015, a selectively-replicating adenovirus, in combination with cisplatin and 5-fluorouracil in patients with recurrent head and neck cancer. Nat Med 2000;6:879–85.
12. Ganly I, Kirn D, Eckhardt G, et al. A phase I study of Onyx-015, an E1B attenuated adenovirus, administered intratumorally to patients with recurrent head and neck cancer. Clin Cancer Res 2000;6:798–806.
13. Dai Y, Schwarz EM, Gu D, Zhang WW, Sarvetnick N, Verma IM. Cellular and humoral immune responses to adenoviral vectors containing factor IX gene: tolerization of factor IX and vector antigens allows for long-term expression. Proc Natl Acad Sci U S A 1995;92:1401–5.
14. Yang Y, Jooss KU, Su Q, Ertl HC, Wilson JM. Immune responses to viral antigens versus transgene product in the elimination of recombinant adenovirus-infected hepatocytes *in vivo*. Gene Ther 1996;3:137–44.
15. Goodrum F, Ornelles D. p53 status does not determine outcome of E1B 55-kilodalton mutant adenovirus lytic infection. J Virol 1998;72:9479–90.
16. Rothmann T, Hengstermann A, Whitaker N, Scheffner M, zur Hausen H. Replication of ONYX-015, a potential anticancer adenovirus, is independent of p53 status in tumor cells. J Virol 1998;72:9470–8.
17. Harada J, Berk A. p53-Independent and -dependent requirements for E1-55K in adenovirus type 5 replication. J Virol 1999;73:5333–44.
18. Logg CR, Logg A, Matusik R, Bochner B, Kasahara N. Tissue-specific transcriptional targeting of a replication-competent retroviral vector. J Virol 2002;76:12783–91.
19. Logg CR, Tai CK, Logg A, Anderson W, Kasahara N. A uniquely stable replication-competent retrovirus vector achieves efficient gene delivery *in vitro* and in solid tumors. Hum Gene Ther 2001;12:921–32.
20. Logg CR, Logg A, Tai CK, Cannon PM, Kasahara N. Genomic stability of murine leukemia viruses containing insertions at the Env-3′ untranslated region boundary. J Virol 2001;75:6989–98.
21. Wang W, Tai CK, Kasahara N, Chen T. Highly efficient and tumor-restricted gene transfer to malignant gliomas by replication-competent retroviral vectors. Hum Gene Ther 2003;14:117–27.
22. Trajcevski S, Solly SK, Frisén C, Trenado A, Cosset FL, Klatzmann D. Characterization of a semi-replicative gene delivery system allowing propagation of complementary defective retroviral vectors. J Gene Med 2005;7:276–87.
23. Tai CK, Wang WJ, Chen TC, Kasahara N. Single-shot, multicycle suicide gene therapy by replication-competent retrovirus vectors achieves long-term survival benefit in experimental glioma. Mol Ther 2005;12:842–51.
24. Solly S, Trajcevski S, Frisén C, et al. Replicative retroviral vectors for cancer gene therapy. Cancer Gene Ther 2003;10:30–9.
25. Hurford RJ, Dranoff G, Mulligan R, Tepper R. Gene therapy of metastatic cancer by *in vivo* retroviral gene targeting. Nat Genet 1995;10:430–5.
26. Kozlowski JM, Fidler IJ, Campbell D, Xu ZL, Kaighn ME, Hart IR. Metastatic behavior of human tumor cell lines grown in the nude mouse. Cancer Res 1984;44:3522–9.
27. Stuhlmann H, Jaenisch R, Mulligan R. Construction and properties of replication-competent murine retroviral vectors encoding methotrexate resistance. Mol Cell Biol 1989;9:100–8.
28. Reik W, Weiher H, Jaenisch R. Replication-competent Moloney murine leukemia virus carrying a bacterial suppressor tRNA gene: selective cloning of proviral and flanking host sequences. Proc Natl Acad Sci U S A 1985;82:1141–5.
29. Goff S, Traktman P, Baltimore D. Isolation and properties of Moloney murine leukemia virus mutants: use of a rapid assay for release of virion reverse transcriptase. J Virol 1981;38:239–48.
30. Alves A, Charre L, Panis Y, et al. Total vascular exclusion of the liver enhances the efficacy of retroviral-mediated associated thymidine kinase and interleukin-2

genes transfer against multiple hepatic tumors in rats. Surgery 2003;133:669–77.

31. Caruso M, Panis Y, Gagandeep S, Houssin D, Salzmann J, Klatzmann D. Regression of established macroscopic liver metastases after *in situ* transduction of a suicide gene. Proc Natl Acad Sci U S A 1993;90:7024–8.

32. Kozak C, Ruscetti S, Levy J. Retroviruses in rodents. In: Levy J, editor. The Retroviridae. New York: Plenum Press; 1992. p. 405–80.

33. Cornetta K, Moen R, Culver K, et al. Amphotropic murine leukemia retrovirus is not an acute pathogen for primates. Hum Gene Ther 1990;1:15–30.

34. Kantoff P, Gillio A, McLachlin J, et al. Expression of human adenosine deaminase in nonhuman primates after retrovirus-mediated gene transfer. J Exp Med 1987;166:219–34.

35. Kasahara N, Dozy AM, Kan YW. Tissue-specific targeting of retroviral vectors through ligand-receptor interactions. Science 1994;266:1373–6.

36. Peng KW, Morling FJ, Cosset FL, Murphy G, Russell SJ. A gene delivery system activatable by disease-associated matrix metalloproteinases. Hum Gene Ther 1997;8:729–38.

37. Diaz R, Eisen T, Hart I, Vile R. Exchange of viral promoter/enhancer elements with heterologous regulatory sequences generates targeted hybrid long terminal repeat vectors for gene therapy of melanoma. J Virol 1998;72:789–95.

38. Ferrari G, Salvatori G, Rossi C, Cossu G, Mavilio F. A retroviral vector containing a muscle-specific enhancer drives gene expression only in differentiated muscle fibers. Hum Gene Ther 1995;6:733–42.

39. Jäger U, Zhao Y, Porter C. Endothelial cell-specific transcriptional targeting from a hybrid long terminal repeat retrovirus vector containing human prepro-endothelin-1 promoter sequences. J Virol 1999;73: 9702–9.

40. Humphreys M, Ghaneh P, Greenhalf W, et al. Hepatic intra-arterial delivery of a retroviral vector expressing the cytosine deaminase gene, controlled by the CEA promoter and intraperitoneal treatment with 5-fluorocytosine suppresses growth of colorectal liver metastases. Gene Ther 2001;8: 1241–7.

41. Li Y, Chen Y, Dilley J, et al. Carcinoembryonic antigen-producing cell-specific oncolytic adenovirus, OV798, for colorectal cancer therapy. Mol Cancer Ther 2003;2:1003–9.

42. Mullen J, Kasuya H, Yoon S, et al. Regulation of herpes simplex virus 1 replication using tumor-associated promoters. Ann Surg 2002;236:502–12.

43. Zhang M, Li S, Nyati M, et al. Regional delivery and selective expression of a high-activity yeast cytosine deaminase in an intrahepatic colon cancer model. Cancer Res 2003;63:658–63.

44. Ueda K, Iwahashi M, Nakamori M, et al. Improvement of carcinoembryonic antigen-specific prodrug gene therapy for experimental colon cancer. Surgery 2003;133:309–17.

Tumor-Selective Gene Expression in a Hepatic Metastasis Model after Locoregional Delivery of a Replication-Competent Retrovirus Vector

Kei Hiraoka, Takahiro Kimura, Christopher R. Logg, et al.

Updated version	Access the most recent version of this article at: http://clincancerres.aacrjournals.org/content/12/23/7108

Cited articles	This article cites 43 articles, 21 of which you can access for free at: http://clincancerres.aacrjournals.org/content/12/23/7108.full#ref-list-1
Citing articles	This article has been cited by 4 HighWire-hosted articles. Access the articles at: http://clincancerres.aacrjournals.org/content/12/23/7108.full#related-urls

E-mail alerts	Sign up to receive free email-alerts related to this article or journal.
Reprints and Subscriptions	To order reprints of this article or to subscribe to the journal, contact the AACR Publications Department at pubs@aacr.org.
Permissions	To request permission to re-use all or part of this article, use this link http://clincancerres.aacrjournals.org/content/12/23/7108. Click on "Request Permissions" which will take you to the Copyright Clearance Center's (CCC) Rightslink site.